

Article

The correlation of coronary flow velocity deficiency and fractional flow reserve in estimating the severity of coronary artery stenosis- a pilot study with preliminary data

Hsu-Ping Wu¹, Cheng-Ting Tsai^{2,3}, Lawrence Yu-Min Liu^{1,4}, Ying-Hsiang Lee^{2,4,5}, Chun-Che Huang⁶, Po-Lin Lin^{1,*}

¹ Division of Cardiology, Hsinchu MacKay Memorial Hospital, Hsinchu, Taiwan

² Cardiovascular Center, MacKay Memorial Hospital, Taipei 104217, Taiwan

³ Department of Cosmetic Applications and Management, MacKay Junior College of Medicine, Nursing and Management, Taipei 25245, Taiwan

⁴ Department of Medicine, MacKay Medical College, New Taipei City 25245, Taiwan

⁵ Department of Artificial Intelligence and Medical Application, MacKay Junior College of Medicine, Nursing and Management, Taipei 25245, Taiwan

⁶ Department of Healthcare Administration, I-Shou University, Kaohsiung, Taiwan

* Dr. Po-Lin Lin, Division of Cardiology, Hsinchu MacKay Memorial Hospital; No. 690, Sec. 2, Guangfu Rd., East Dist., Hsinchu City 30041, Taiwan (R.O.C.); Tel: +886-3-6119595; E-mail: Berlin831@gmail.com

Accepted 1 January 2023; Volume: 5; Issue: 1; Pages: 1-9; DOI: [10.6907/SCJ.202301_5\(1\).0001](https://doi.org/10.6907/SCJ.202301_5(1).0001)

Abstract:

Fractional flow reserve (FFR) is a current standard method for estimating myocardial ischemia. It involves measuring the pressure differences across a coronary artery stenosis, but this requires the use of an invasive pressure wire. According to Poiseuille's law, there may be a correlation between coronary pressure gradient and coronary flow velocity. With this in mind, our goal was to investigate whether coronary flow velocity deficiency (CFVD) could be detected using routine angiographic images, and to examine its relationship with FFR. We enrolled 14 individuals who underwent coronary angiography with FFR measurement. Among the 14 de-novo lesions collected, 7 were from the left anterior descending artery, 3 from the left circumflex artery, and 4 from the right coronary artery. The CFVD was determined by calculating the ratio of post-stenosis contrast length to pre-stenosis contrast length. We collected data on various lesion characteristics, including gender, age, vessel lesion, ECG rhythm, adenosine dose (ug), FFR, and pre- and post-stenosis contrast length (mm/frame). All lesions were divided into two groups based on pre- and post-adenosine status, and were compared with individual FFR measurements. Significant differences were observed between pre- and post-adenosine measurements of FFR (0.953 ± 0.036 , 0.896 ± 0.069 , $P=0.01$), CFVD (0.958 ± 0.039 , 0.895 ± 0.076 , $P=0.01$), pre-stenosis length ($10.02 \pm 4.20\text{mm}$, $14.74 \pm 4.95\text{mm}$, $P=0.01$), and post-stenosis length ($9.58 \pm 3.91\text{mm}$, $13.14 \pm 3.88\text{mm}$, $P=0.02$). The Pearson correlation coefficients for FFR and CFVD were 0.836 and 0.894 for pre- and post-adenosine measurements, respectively. Conclusion: There was a high correlation between CFVD and both pre- and post-adenosine FFR measurements, suggesting that CFVD could be a useful pre-FFR test for predicting the severity of myocardial ischemia before using invasive FFR.

Citation: str.circ.j., 2023, 5, 1, 1, 1-9

1. Introduction

Cardiovascular disease, particularly coronary artery disease (CAD), continues to be the leading cause of morbidity and mortality worldwide, despite advancements in medication and diagnostic tools [1]. The rising prevalence of CAD has made it a major contributor to increasing healthcare costs [2]. While invasive coronary angiography (CAG) is considered the gold standard for anatomical detection of obstructive CAD, it often overestimates the severity of coronary stenosis and underestimates lesion length [3]. Moreover, CAG alone cannot accurately determine the hemodynamic significance of coronary lesions, especially those of intermediate stenosis severity [4]. Morphological luminal narrowing of the coronary artery on CAG doesn't always cause myocardial ischemia, particularly in the case of intermediate stenosis severity [4,5]. Fractional flow reserve (FFR), an alternative pressure-derived estimate of coronary flow impairment, has been shown to be a better option than CAG alone for determining the hemodynamic significance of stenosis and reducing morbidity and cost of care in patients with intermediate-grade stenosis [6]. A recent clinical study has demonstrated that FFR is an independent prognostic factor in patients with CAD and is considered the gold standard for decision-making in percutaneous coronary intervention [7]. However, FFR is another invasive tool for CAD detection and can increase other medical costs with some inherent risks [8].

Noninvasive technologies, such as coronary computed tomography angiography (CCTA), fractional flow reserve derived from coronary computed tomography angiography (FFRCT), virtual reality, or vascular robotic systems, are being developed to improve the diagnosis of CAD and identify vulnerable plaque before percutaneous treatment strategies [9]. Current guidelines recommend CCTA for excluding obstructive CAD in patients with low-to-intermediate cardiovascular risk due to its high negative predictive value [10]. However, the lower positive predictive value and overestimation of coronary lesion severity are clinical limitations of CCTA [11]. Non-invasive FFR derived from CCTA (called FFRCT) may provide incremental diagnostic value over CCTA alone by combining anatomic and functional information [12]. Recent studies show the high discriminatory accuracy of FFRCT in detecting hemodynamically significant stenosis compared to invasive FFR, and additional functional parameters obtained from FFRCT may enhance diagnostic performance when detecting hemodynamically significant CAD [10]. In addition, FFRCT could provide additional markers, including plaque morphology, volume, and composition, compared to invasive coronary angiography alone [10]. However, the major disadvantages of FFRCT include the need for a separate test and the time-consuming process of transforming CCTA to FFRCT, making it challenging to determine the hemodynamic relevance of anatomic coronary artery stenosis in FFRCT.

Our research focuses on the clinical impact of non-invasive modalities based on the mechanism of FFR, which may improve the diagnostic rate of CAD without increasing further medical costs. FFR is the ratio of hyperemic myocardial blood flow in the presence of stenosis to hyperemic flow in the absence of stenosis [13]. Blood flow through a vessel is measured by the change in pressure divided by resistance. After adjusting flow resistance by adenosine and ignoring smaller venous pressure, the final FFR is the ratio of pre- and post-stenotic pressure gradient [13]. According to Poiseuille's law, coronary flow velocity correlates with coronary pressure gradient when there is a similar vessel diameter and smaller stenotic length [14]. The objective of our study was to test the feasibility of detecting coronary flow deficiency (CFVD) using routine angiographic images and find the clinical correlation with FFR.

2. Methods and Materials

2.1. Study population

This retrospective study included patients who underwent elective CAG and clinically indicated FFR testing between July 2019 and March 2020. Enrolled lesions had intermediate stenosis (50% to 69% by quantitative assessment). To be eligible, patients had relatively simple naïve vessel coronary disease (ideally Type A lesions) or were scheduled to undergo clinically non-emergent CAG. FFR was

measured in one or more coronary arteries in each patient as per the attending physician's decision. Patients were excluded if they had unstable coronary anatomy such as left main disease or chronic total occlusion, could not receive intracoronary nitrate, had a known anaphylactic reaction to iodinated contrast, or had contraindications to intracoronary adenosine (including second- or third-degree heart block, sick sinus syndrome, long QT syndrome, severe hypotension, severe asthma, or severe or bronchodilator-dependent chronic obstructive pulmonary disease). The Mackay hospital Institutional Review Board approved this study (19MMHIS124e).

2.2. Procedure protocol-FFR

Rotational coronary angiography (RoCA) was conducted using a bi-plane axis (SIEMENS, Artis Zee Biplane) after iso-centering in the posterior-anterior and lateral planes (as close to 90° apart as possible). Angiographic views were obtained after administering intra-coronary isosorbide dinitrate (100 or 200 µg) for its vasodilatory effect. To ensure optimal vessel opacification, a hand injection of 10 to 20 ml contrast was administered through a 6- or 7-F guiding catheter. FFR testing was indicated for intermediate stenosis (50% to 69% by quantitative assessment) in accordance with Taiwan's National Health Insurance recommendation. Following the "equalizing" of the pressure wire sensor at the guiding catheter tip, a pressure-sensitive angioplasty wire (Volcano, PrimeWire PRESTIGE / St. Jude medical, Pressure Wire "Certus") was advanced distal to the stenosis. Hyperemia was induced by an intra-coronary infusion of adenosine at 48 µg for the right coronary artery (RCA) and 240 to 480 µg for the left anterior descending artery (LAD) and left circumflex artery (LCX). After maximal hyperemia and vasodilatation by adenosine and nitrate, FFR could be estimated 3 to 5 seconds later, and its FFR result was recorded as the gold standard.

2.3. Procedure protocol-CFVD

Based on the mechanism of FFR, it is the ratio of hyperemic myocardial blood flow in the presence of a stenosis to hyperemic flow in the absence of a stenosis [13]. The blood flow through a vessel can be measured by the change in pressure divided by resistance. After reducing coronary resistance and inducing coronary hyperemia by intra-coronary adenosine, and ignoring smaller venous pressure, the final FFR can be determined by the ratio of the pre- and post-stenotic pressure gradient. According to Poiseuille's law, the coronary flow velocity may correlate with the coronary pressure gradient if the vessel diameter and the stenotic length are similar (Fig. 1) [14]. In our study, we selected a short distance around the target stenotic area (within 1-3 frames), while the diameter of the vessel was relatively similar within the stenotic area. Therefore, we hypothesized that there could be a correlation between coronary flow velocity and coronary pressure gradient if the parameters of Poiseuille's equation were similar within a focal stenotic lesion.

$$Q = \frac{\pi Pr^4}{8\eta l}$$

Figure 1. Poiseuille's equation. R = inside radius of tube, L=length of tube, P= pressure difference between ends, η = the coefficient of viscosity, and Q=the volume rate of flow

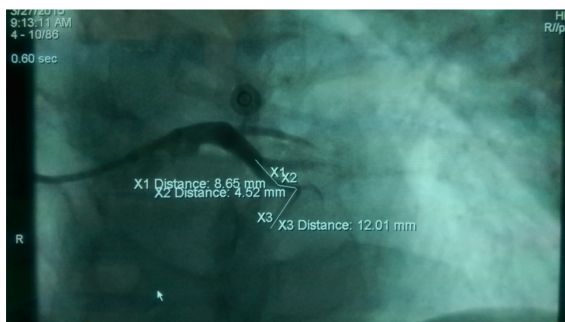
After performing invasive FFR testing, the collection of images for "CFVD" was carried out: A hand injection of 10 to 20 ml contrast was administered through a 6- or 7-F guiding catheter after inducing maximum hyperemia (10 seconds later) using intra-coronary adenosine (at the same dosage as in the FFR testing). The distances of the same contrast frame before and after the stenotic lumen were calculated by the radiologist after the procedure. CFVD was calculated by dividing the contrast distance after the stenosis by the contrast distance before the stenosis (as shown in Fig. 2A). The frame time (1/30 seconds per X-ray frame) was the same for both before and after stenosis distances calculated. CFVD was determined with and without adenosine images, as described in Fig. 2B and

2C. We compared the clinical accuracy of CFVD with FFR, using the standard value of FFR with and without adenosine.

(A)

$$\text{Coronary flow velocity deficiency (CFVD)} = \frac{\text{Post-stenosis length (mm)}}{\text{Pre-stenosis length (mm)}}$$

(B)



(C)

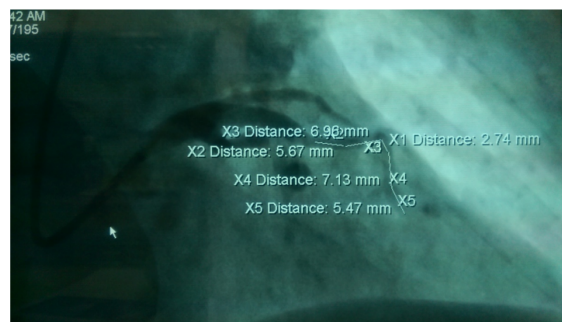


Figure 2. (A) Our hypothesis of CFVD to predict the myocardial ischemia status, compared with the golden standard of FFR data. (B) Compared pre-adenosine CFVD and FFR. In the case of LAD, the middle segment with 55% stenosis. The standard value of resting FFR was 0.94. The CFVD (0.91) was calculated from 12.01mm divided by 8.65+8.52mm. (C) Compared post-adenosine CFVD and FFR. In the same case of LAD, the middle segment with 55% stenosis. The standard value of post-hyperemia FFR was 0.84. The post-hyperemia CFVD (0.81) was calculated from 7.13+5.47 mm divided by 5.67+6.96+2.74 mm.

2.4. Statistical analysis

Clinical characteristics were analyzed on a per-patient basis, while other factors were analyzed on a per-vessel basis. Pearson correlation was used to assess the clinical relationship between standard FFR and CFVD in both pre- and post-adenosine conditions among the 14 patients. The data analyses were conducted using IBM SPSS Statistics 24.0 for Windows (IBM Corp., Chicago, IL, USA).

3. Results

3.1. Patient and clinical characteristics

Fourteen patients with anatomical and physiological datasets matched were included in the study, with 7 having left LAD, 3 having LCX, and 4 having RCA. The baseline characteristics of the study patients, such as age, gender, and heart rhythm, were recorded and presented in Table 1. The mean age of the group was 59 years (range 44 to 86), and 12 vessels were male-predominant (86%). None of the patients had a prior history of coronary disease or stent implantation. Two vessels were indicated for stent implantation after measuring FFR. The lesion characteristics, including gender, age, vessel lesion, heart rhythm, adenosine dose (µg), FFR value (pre- and post-adenosine), pre- and post-adenosine peri-stenosis contrast length (mm), and pre- and post-adenosine peri-stenosis CFVD, are detailed in Table 2.

Table 1. Baseline characteristics of all hypertensive patients and patients treated with thiazide diuretics as add-on therapy or monotherapy

Age	Mean 59 y/o (44 -86 age)
Gender	
Male	12
Female	2
Lesion territory	
LAD	7
LCX	3
RCA	4
Heart rhythm	
NSR	13
Atrial fibrillation (AF)	1
FFR (Pre-adenosine)	0.953±0.036
FFR (Post-adenosine)	0.896±0.069

LAD, left anterior descending artery; LCX, left circumflex artery; RCA, right coronary artery; NSR, normal sinus rhythm; FFR, fractional flow reserve.

Table 2. Characteristics of each study vessel and individual FFR/ CFVD.

No.	Gender Age	Vessel Lesion (Stenosis%)	Heart rhythm	FFR		Adenosine Dose (µg)	Contrast length (mm/frame)		CFVD	Contrast length (mm/frame)		CFVD
				Pre- adenosine	Post- adenosine		Pre- stenosis	Post- stenosis		Pre- stenosis	Post- stenosis	
1	M 52	M-LAD 50%	NSR	0.94	0.89	480	5.99	5.8	0.96	8.27	7.58	0.91
2	M 44	M-RCA 60%	NSR	0.98	0.91	48	9.36	9.26	0.98	16.18	15.29	0.94
3	F 62	P- LAD 58%	NSR	0.95	0.88	240	19.39	18.75	0.96	24.02	20.94	0.87
4	F 62	P- LCX 55%	NSR	0.95	0.88	240	8.42	8.02	0.95	12.14	11.2	0.92
5	M 53	M-LAD 60%	NSR	0.92	0.79	480	8.38	7.86	0.93	14.07	12.57	0.81
6	M 86	M-LCX 55%	NSR	0.94	0.93	240	9.38	9.19	0.97	11.68	11.29	0.96
7	M 86	M-LAD 30%	NSR	0.87	0.84	240	13.42	11.51	0.85	13.41	11.3	0.84
8	M 65	P-LAD 60%	NSR	0.93	0.75	240	16.16	15.58	0.96	23.48	16.79	0.72
9	M 39	M-RCA 52%	NSR	1.00	0.99	48	6.52	6.49	0.99	10.83	10.01	0.92
10	M 59	D-LCX 60%	NSR	1.00	0.99	240	6.26	6.21	0.99	9.62	9.48	0.99
11	M 59	M-LAD 35%	NSR	0.95	0.92	240	9.08	9.01	0.99	11.11	10.55	0.95
12	M 49	M-RCA 52%	NSR	0.98	0.95	48	4.33	4.30	0.99	20.97	19.7	0.94
13	M 58	M-LAD 55%	AF	0.94	0.87	240	13.17	12.01	0.91	15.37	12.6	0.81
14	M 61	M-RCA 55%	NSR	1.00	0.95	240	10.36	10.10	0.97	15.27	14.68	0.96

Gender (M: male; F: female); Vessel lesion (P: proximal, M: middle, D: distal); NSR, normal sinus rhythm; LAD, left anterior descending artery; LCX, left circumflex artery; RCA, right coronary artery; FFR, fractional flow reserve.

Table 3. Correlation in pre-and post-adenosine FFR, CFVD, pre- and post-stenosis length.

	Pre-adenosine	Post-adenosine	P valve
FFR	0.953±0.036	0.896±0.069	0.01
CFVD	0.958±0.039	0.895±0.076	0.01
Pre-stenosis contrast length(mm)	10.02±4.2	14.74±4.95	0.01
Post-stenosis contrast length(mm)	9.58±3.91	13.14±3.88	0.02

3.2. Correlation between FFR and CFVD

The lesions were divided into two groups: pre-adenosine and post-adenosine status. The CFVD was also stratified in the same way, and the results were compared with FFR. Significant differences were observed in pre- and post-adenosine FFR (0.953±0.036, 0.896±0.069, P=0.01), CFVD (0.958±0.039, 0.895±0.076, P=0.01), pre-stenosis contrast length (10.02±4.20mm, 14.74±4.95mm, P=0.01), and post-stenosis contrast length (9.58±3.91mm, 13.14±3.88mm, P=0.02) (see Table 3). The Pearson correlation coefficient between the pre-adenosine FFR values and the pre-adenosine CFVD values was 0.836 (Fig. 3A). Likewise, the Pearson correlation coefficient between the post-adenosine FFR values and the post-adenosine CFVD values was 0.894 (Fig. 3B). The individual FFR was compared with its corresponding CFVD in two groups of pre-adenosine and post-adenosine in Fig. 4A and B.

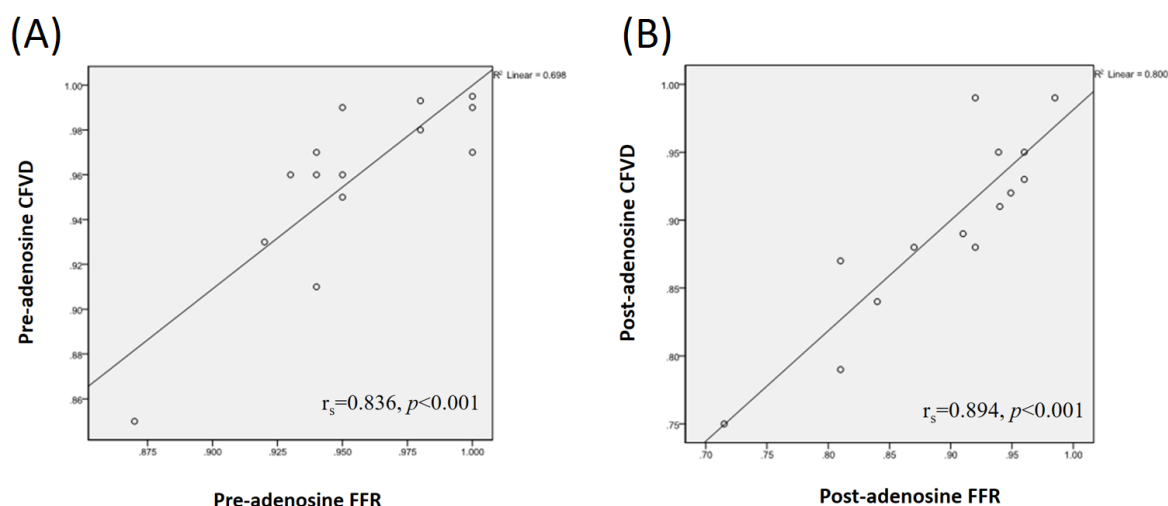


Figure 3. (A) Pearson correlation for pre-adenosine FFR and CFVD: $r_s=0.836$, $p<0.001$. (B) Pearson correlation for post-adenosine FFR and CFVD: $r_s=0.894$, $p<0.001$.

4. Discussion

Coronary anatomical data alone is insufficient for predicting the physiological significance of myocardial ischemia [15]. To address this, we developed a simple coronary workflow that utilizes image analysis to predict clinically useful physiological measures within a diseased coronary circulation, using only angiographic images. Our workflow generates a simplified 2D virtual coronary image from a single RoCA, and unlike previous detection tools, our model doesn't require data on generic boundary conditions, blood pressure, or flow solution. The CFVD method used in our workflow allows for the assessment of one or more coronary stenosis during estimation. The pre-adenosine FFR values were found to be closely correlated with pre-adenosine CFVD values, with a Pearson correlation coefficient of 0.836. The correlation coefficient was even higher for post-adenosine FFR values with post-adenosine CFVD values, at 0.894, exceeding that of pre-adenosine CFVD.

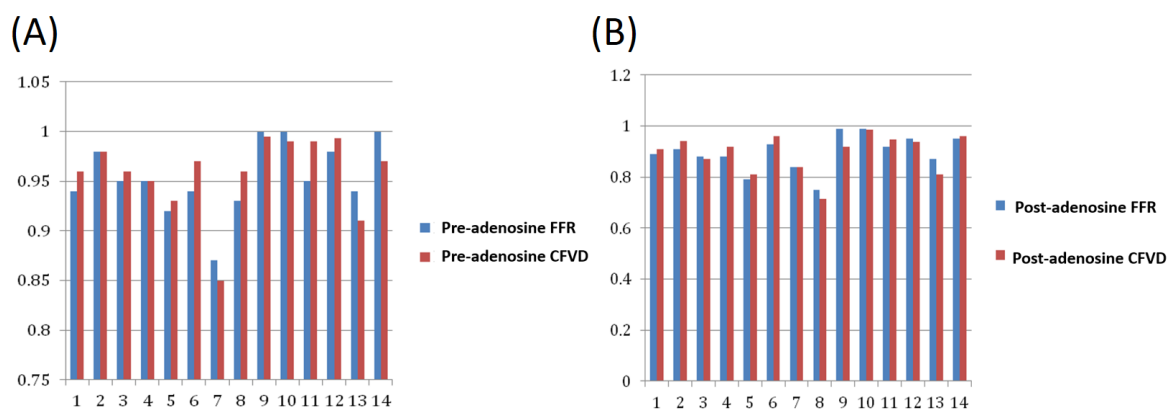


Figure 4. (A) Each vessel's re-adenosine FFR (blue) compared with CFVD (red). (B) Each vessel's post-adenosine FFR (blue) compared with CFVD (red).

Previous research on FFR and virtual FFR has focused on the 3D anatomic reconstruction of the entire vessel, from proximal to distal, under continuous hyperemia induced by intravenous adenosine [4]. However, this method is time-consuming for longer vessels with both significant and non-significant stenosis, and is associated with higher procedural costs, including the use of a higher dose of intravenous adenosine. To address these limitations, we used intracoronary bolus adenosine for immediate hyperemia induction with a short-acting time and measured the FFR difference in focal coronary stenosis. A good correlation between intracoronary bolus and continuous intravenous adenosine has been noted in the past, except for tandem or diffuse lesions [16]. We also used the intracoronary bolus adenosine route for the RoCA image and CFVD estimation, compared to FFR via intracoronary bolus adenosine. During adenosine-induced maximal hyperemia, there is an increase in both coronary blood flow and trans-stenotic pressure gradient in both phases of the cardiac cycle [17]. This explains why there were significant contrast length differences in pre- and post-stenosis after intra-coronary adenosine infusion, compared to the pre-adenosine status. The increase in coronary flow with trans-stenotic pressure after maximal hyperemia is an essential step, and we found a higher correlation between FFR and CFVD in the post-adenosine group.

Estimating FFR is challenging due to microcirculatory resistance. Changes in downstream microcirculation resistance can limit the increase in blood flow after vasodilation, which can restrict the pressure drop downstream of the stenosis in the epicardial artery, leading to an inadequate drop in pressure [4]. This can decrease the velocity deficiency of coronary flow, resulting in an overestimation of CFVD as a smaller velocity deficiency. Consequently, the severity of the stenosis may be underestimated if the resistance is high. Previous attempts to predict the physiological significance of CAD from luminal geometry using quantitative coronary angiography, intravascular ultrasound, and optical coherence tomography have yielded disappointing results [4,6,18]. Our methodology only requires knowledge of the vessel's geometry without considering boundary conditions based on multiple arterial resistance or compliance measurements and a Windkessel model [19].

Our CFVD workflow offers several advantages when using physiological measures. The model only requires knowledge of vessel geometry, eliminating the need for additional procedure time, intracoronary wire passage, extra equipment, training, or cost. However, the CFVD model may overestimate or underestimate length in cases of poor-quality coronary images or tortuous vessels. For instance, in case 13, the post-adenosine CFVD values (0.81) were smaller than the post-adenosine FFR values (0.87). The irregularity of the heartbeat may have affected the CFVD estimate, causing a discrepancy between CFVD and FFR measurements.

There are a few potential limitations to this study. First, the sample size was small as the study was conducted in a single institution, and this may limit the ability to demonstrate a linear correlation. However, the results are promising and suggest the need for larger studies. Second, due to the limited number of images taken at end diastole during coronary angiography, the model may require 3D

reconstruction of coronary flow velocity using an automated contrast injector to improve its clinical indications and effectiveness in more complex cases. Third, the majority of lesions in the study were intermediate in appearance, and only a limited subgroup of cases (n=2) had FFR values falling between 0.70 and 0.80.

In conclusion, our study showed that CFVD had a highly positive correlation with FFR, suggesting that it could potentially serve as a pre-FFR test. In combination with other invasive or non-invasive tools, CFVD may enhance the accuracy of predicting myocardial ischemia on an individual basis.

Conflicts of Interest:

The authors declare no conflict of interest.

References

1. Komajda, M.; Weidinger, F.; Kerneis, M.; Cosentino, F.; Cremonesi, A.; Ferrari, R.; Kownator, S.; Steg, P.G.; Tavazzi, L.; Valgimigli, M.; others. EURObservational research programme: the chronic ischaemic cardiovascular disease registry: Pilot phase (CICD-PILOT). *European heart journal* **2016**, *37*, 152–160.
2. Song, X.; Quek, R.G.; Gandra, S.R.; Cappell, K.A.; Fowler, R.; Cong, Z. Productivity loss and indirect costs associated with cardiovascular events and related clinical procedures. *BMC health services research* **2015**, *15*, 1–14.
3. Green, N.E.; Chen, S.Y.J.; Messenger, J.C.; Groves, B.M.; Carroll, J.D. Three-dimensional vascular angiography. *Current problems in cardiology* **2004**, *29*, 104–142.
4. Morris, P.D.; Ryan, D.; Morton, A.C.; Lycett, R.; Lawford, P.V.; Hose, D.R.; Gunn, J.P. Virtual fractional flow reserve from coronary angiography: modeling the significance of coronary lesions: results from the VIRTU-1 (VIRTUal Fractional Flow Reserve From Coronary Angiography) study. *JACC: Cardiovascular Interventions* **2013**, *6*, 149–157.
5. Pijls, N.H.; van Schaardenburgh, P.; Manoharan, G.; Boersma, E.; Bech, J.W.; van't Veer, M.; Bär, F.; Hoorntje, J.; Koolen, J.; Wijns, W.; others. Percutaneous coronary intervention of functionally nonsignificant stenosis: 5-year follow-up of the DEFER Study. *Journal of the American College of Cardiology* **2007**, *49*, 2105–2111.
6. Abdulla, J.; Abildstrom, S.Z.; Gotzsche, O.; Christensen, E.; Kober, L.; Torp-Pedersen, C. 64-multislice detector computed tomography coronary angiography as potential alternative to conventional coronary angiography: a systematic review and meta-analysis. *European heart journal* **2007**, *28*, 3042–3050.
7. Knuuti, J.; Revenco, V. 2019 ESC Guidelines for the diagnosis and management of chronic coronary syndromes. *European heart journal* **2020**, *41*, 407–477.
8. Levine, G.N.; Bates, E.R.; Blankenship, J.C.; Bailey, S.R.; Bittl, J.A.; Cercek, B.; Chambers, C.E.; Ellis, S.G.; Guyton, R.A.; Hollenberg, S.M.; others. 2015 ACC/AHA/SCAI focused update on primary percutaneous coronary intervention for patients with ST-elevation myocardial infarction: an update of the 2011 ACCF/AHA/SCAI guideline for percutaneous coronary intervention and the 2013 ACCF/AHA guideline for the management of ST-elevation myocardial infarction: a report of the American College of Cardiology/American Heart Association Task Force on Clinical Practice Guidelines and the Society for Cardiovascular Angiography and Interventions. *Circulation* **2016**, *133*, 1135–1147.
9. Dugas, C.M.; Schussler, J.M. Advanced technology in interventional cardiology: a roadmap for the future of precision coronary interventions. *Trends in cardiovascular medicine* **2016**, *26*, 466–473.
10. Tesche, C.; De Cecco, C.N.; Caruso, D.; Baumann, S.; Renker, M.; Mangold, S.; Dyer, K.T.; Varga-Szemes, A.; Baquet, M.; Jochheim, D.; others. Coronary CT angiography derived morphological and functional quantitative plaque markers correlated with invasive fractional flow reserve for detecting hemodynamically significant stenosis. *Journal of cardiovascular computed tomography* **2016**, *10*, 199–206.
11. Budoff, M.J.; Nakazato, R.; Mancini, G.J.; Gransar, H.; Leipsic, J.; Berman, D.S.; Min, J.K. CT angiography for the prediction of hemodynamic significance in intermediate and severe lesions: head-to-head comparison with quantitative coronary angiography using fractional flow reserve as the reference standard. *JACC: Cardiovascular Imaging* **2016**, *9*, 559–564.
12. Budde, R.P.; Nous, F.M.; Roest, S.; Constantinescu, A.A.; Nieman, K.; Brugts, J.J.; Koweek, L.M.; Hirsch, A.; Leipsic, J.; Manintveld, O.C. CT-derived fractional flow reserve (FFR_{CT}) for functional coronary artery evaluation in the follow-up of patients after heart transplantation. *European Radiology* **2021**, pp. 1–10.

13. Osawa, K.; Miyoshi, T.; Miki, T.; Koyama, Y.; Sato, S.; Kanazawa, S.; Ito, H. Diagnostic performance of first-pass myocardial perfusion imaging without stress with computed tomography (CT) compared with coronary CT angiography alone, with fractional flow reserve as the reference standard. *PloS one* **2016**, *11*, e0149170.
14. Hirshfeld Jr, J.W.; Nathan, A.S. Deriving function from structure: applying Hagen-Poiseuille to coronary arteries, 2020.
15. Davies, J.E.; Whinnett, Z.I.; Francis, D.P.; Manisty, C.H.; Aguado-Sierra, J.; Willson, K.; Foale, R.A.; Malik, I.S.; Hughes, A.D.; Parker, K.H.; others. Evidence of a dominant backward-propagating “suction” wave responsible for diastolic coronary filling in humans, attenuated in left ventricular hypertrophy. *Circulation* **2006**, *113*, 1768–1778.
16. Schlundt, C.; Bietau, C.; Klinghammer, L.; Wiedemann, R.; Rittger, H.; Ludwig, J.; Achenbach, S. Comparison of intracoronary versus intravenous administration of adenosine for measurement of coronary fractional flow reserve. *Circulation: Cardiovascular Interventions* **2015**, *8*, e001781.
17. Härle, T.; Bojara, W.; Meyer, S.; Elsässer, A. Comparison of instantaneous wave-free ratio (iFR) and fractional flow reserve (FFR)—first real world experience. *International journal of cardiology* **2015**, *199*, 1–7.
18. Gonzalo, N.; Escaned, J.; Alfonso, F.; Nolte, C.; Rodriguez, V.; Jimenez-Quevedo, P.; Bañuelos, C.; Fernández-Ortiz, A.; Garcia, E.; Hernandez-Antolin, R.; others. Morphometric assessment of coronary stenosis relevance with optical coherence tomography: a comparison with fractional flow reserve and intravascular ultrasound. *Journal of the American College of Cardiology* **2012**, *59*, 1080–1089.
19. Aboelkassem, Y.; Virag, Z. A hybrid Windkessel-Womersley model for blood flow in arteries. *Journal of theoretical biology* **2019**, *462*, 499–513.